Preliminary In-Orbit Results of the PRETTY ESA Technology CubeSat

Camille Pirat [(1)], Andreas Hörmer [(2)], Andreas Dielacher [(2,3)], Manuela Wenger [(2)], Michael Moser-Moritsch [(3)], Christoph Tscherne [(4)], Roger Walker [(1)]

[(1)] ESA-ESTEC, Keplerlaan 1, 2201 AZ Noordwijk, Netherlands, camille.pirat@esa.int
[(2)] Graz University of Technology, Rechbauerstraße 12, A-8010 Graz, Austria, hoermer@tugraz.at
[(3)] Beyond Gravity Austria GmbH, Stachegasse 13, Vienna, Austria, andreas.dielacher@beyondgravity.com
[(4)] Seibersdorf Laboratories GmbH, Tech Campus Seibersdorf, 2444 Seibersdorf, Austria, christoph.tscherne@seibersdorf-laboratories.at

ABSTRACT

PRETTY (Passive REflecTometry and dosimeTrY) is a European Space Agency (ESA) In-Orbit Demonstration (IOD) CubeSat funded by Austria under the Fly element of ESA General Support Technology Programme (GSTP), demonstrating for the first time Global Navigation Satellite Systems (GNSS) reflectometry (GNSS-R) at low grazing angles using the E5/L5 frequency, transmitted by the European Galileo and American GPS constellations. It was launched in October 2023 on board VEGA VV23 into a sun-synchronous orbit at 560 km. The GNSS-R payload provides ice and sea ice height measurements to an accuracy of 50 cm, with a special focus on polar regions. PRETTY's second payload, SATDOS-1, is a compact reference dosimeter tailored for CubeSat applications. In this paper, the overall platform architecture and mission design will be presented, followed by the results of the commissioning phase and early scientific data from the two payloads. The platform key telemetry points will be compared against the predictions from analysis work. The overall performances of the VHF link in the Short Duration Mission band will then be provided.

1 INTRODUCTION

PRETTY is a 3U CubeSat launched onboard VEGA VV23 on 9 October 2023 into a 560km Sun Synchronous Orbit. It is a European Space Agency (ESA) In-Orbit Demonstration (IOD) CubeSat funded by Austria under the Fly element of ESA General Support Technology Programme, demonstrating for the first time Global Navigation Satellite Systems (GNSS) reflectometry (GNSS-R) at low grazing angles using the E5/L5 frequency, transmitted by the European Galileo and American GPS constellations. As such, it is also the first GNSS-R mission for ESA. The GNSS-R payload provides ice and sea ice height measurements to an accuracy of 50 cm. The measurements are carried out using the interferometric approach, i.e. correlating the direct and reflected GNSS signals, received simultaneously by the same two patch antennas array. Both antennas are independently fed to a Software-Defined Radio (SDR), which enables beamforming capabilities, allowing the direct and reflected signals to be tracked independently. A novelty of the mission, in addition to using the E5/L5 signals, is the low grazing geometry, which offers significant advantages compared to the classical measurement carried out at the local vertical of the spacecraft. Indeed, in a grazing geometry, the sea appears smoother leading to a reflected signal of greater coherence, enabling longer integration time. PRETTY's second payload, SATDOS-1, is a compact reference dosimeter tailored for CubeSat applications. The platform is outfitted with dose integration enabling the evaluation of mission total ionizing dose (TID), as well as in-orbit single event effects (SEE), which will *in fine* support the reliability and sustainability of future missions on similar orbits. Finally, and even if not specifically a payload, a novelty of PRETTY is its telecommand and telemetry radio link, which makes use of the newly created Short Duration Mission frequency band by the International Telecommunication Union. PRETTY is among the first CubeSat to be using this radio band, located in the VHF part of the spectrum.

PRETTY was developed by an all-Austrian consortium, led by Beyond Gravity Austria, also in charge of the GNSS-R payload development, with Graz University of Technology, as payload hardware developer, system integrator and operator, and with Seibersdorf Laboratories developing the SATDOS. The spacecraft protoflight model was accepted for flight by ESA in December 2022 and was due for launch on VEGA C in March 2023. The project incurred an unexpected delay due to the VV22 failure in December 2022 and subsequent hold of future VEGA C launches. PRETTY was re-manifested on a spare VEGA flight, put in place exceptionally by AVIO and ArianeSpace, and was successfully launched into a Sun Synchronous Orbit at 560 km altitude on 9 October 2023. The IOD mission is planned to last until October 2024 at least.

2 MISSION AND SYSTEM DESCRIPTION

PRETTY is built following the 3U CubeSat form factor. The mission has been built as a technology demonstrator of the GNSS-R and dosimeter payloads. Consequently, the platform has been entirely built out of commercial-off-the-shelf (COTS) components. The platform and payloads have been designed for a lifetime of at least one year, and consequent qualification activities have been included during the payload development to ensure this lifetime, such as total ionizing dose and proton testing (for the GNSS-R payload). Both payloads are designed to be operated fully autonomously and consequently, the overall mission design is relatively straightforward. When doing GNSS-R, PRETTY actively tracks the reflection events as commanded by the payload. This is done at most 30 minutes per day and is being constrained by the data return capabilities. The dosimeter is by default enabled at any given time and only requires regular time synchronisation with the platform on-board computer. The rest of the time, PRETTY is either sun pointing or maintained fixed in the orbital frame. Finally, when above the ground station (on average 5 times per day for a total averaged access time of 22 min), the payloads data and on-board telemetries are being downloaded.

A significant effort was spent on the autonomous selection of the reflection points by the GNSS-R payload. An advanced mission planning tool was developed and allows on-board autonomous selection of the reflection points based on geometry constraints and weighting factors to give preference to certain location (e.g. the poles). This software can also be run on ground to pre-identify reflections of interest. The time stamps of these events are then transferred to the mission operation centre (MOC) and uploaded on-board in the form of time-tagged commands. Both operational options are being used and inputs from the extended scientific consortium are being factored into the operational solution to be used.

PRETTY is composed of the following components:

- Platform subsystems: OBC, ADCS, S-Band, VHF, EPS, GPS
- Payloads: processing engine, software-defined radio (SDR) RF frontend (both making the GNSS-R payload), Dosimeter payload

The ground-segment is composed of the MOC and ground station, both located at TU-Graz in Austria. In addition, the scientific data are being transferred to a shared server accessible by the scientific consortium for the analysis of the in-orbit results.

In depth descriptions of the mission and system design can be found in [1], [2]

2.1 Platform Architecture

An overview of the complete stack is provided in Figure 1.

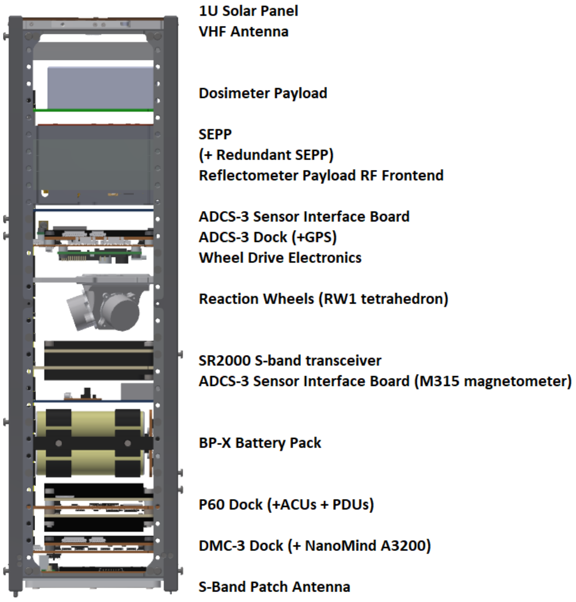

Figure 1 PRETTY stack.

The EPS is composed of a single battery pack, two double deployable solar arrays, body mounted solar panels, two Array Conditioning Units (ACUs) that include the maximum power point tracking, and two Power Distribution Units (PDUs). The overall configuration of the spacecraft is depicted on Figure 2 PRETTY external configuration.Figure 2.

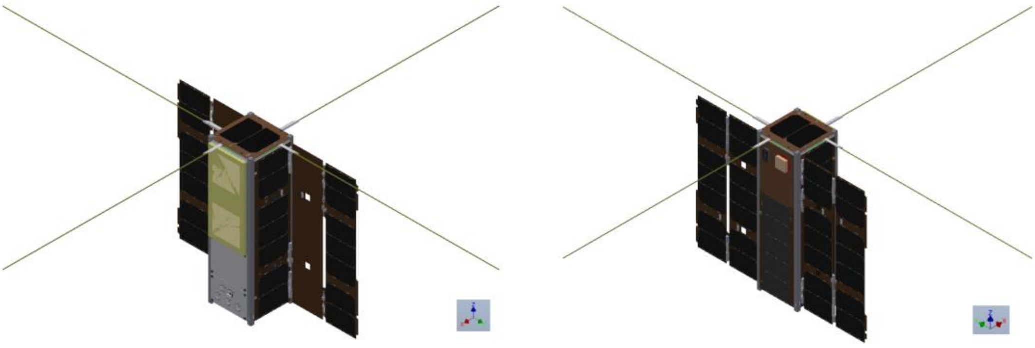

Figure 2 PRETTY external configuration.

When sun-pointing, the spacecraft can generate around 30W peak power. Body mounted cells have been included to ensure a power positive budget even when tumbling in safe mode. It should also be noted that a 20% system margin is kept on the power budget throughout the project lifecycle. The battery has a 77Wh capacity at beginning of life (BoL) and provides an unregulated voltage between 24 V and 32.8V. Both PDUs can provide 3.3V, 5V or 8V (regulated). The EPS contains in addition critical safety functions, such as undervoltage protections, triggering safe and critical modes, as well as ground watchdogs (48hrs timers triggering a reboot of the platform if not reset by telecommand).
The OBC executes the central software but is not required to decode telecommand received the radio or encode telemetries. Thanks to the CAN/CSP architecture of the command and data handling

(C&DH), which will be further described below, the platform remains fully operational even in case of OBC outage. The OBC oversees the flight planer execution (time tagged commands), the Fault Detection, Identification, and Recovery (FDIR), as well as the platform telemetry (TM) logging (except the ADCS ones). The OBC software is off-the-shelf, however, using the provided API, an additional FDIR layer was developed which provides a high level of flexibility into the implementation of new FDIR rules. Briefly, the FDIR allows monitoring any available TM point that are being broadcasted by the various subsystems on the data bus and executing logical tests on them. When a logical test becomes true, a telecommand (TC) can be autonomously executed (such as powering down a PDU channel, power cycling an equipment, switching ADCS mode, …). This functionality has proven extremely useful in orbit and further details are provided in the next section.

The overall C&DH architecture is provided in Figure 3. Each subsystem, including the payloads, are interfaces on a single CAN data bus. A network is then created between the each of the subsystems using the CubeSat Space Protocol (CSP) [3]. The ground station is also acting as nodes nodesa nodea nodda nodoa nod of this CSP network, but accessing it using an RF interface instead of a CAN bus. This distributed architecture has the significant advantage that any subsystems (node) can be independently accessed from ground (TCs are CSP commands that can be decoded by any node of the network) and hence offers a significant functional redundancy, as opposed to centralised architectures in which the OBC would need to decode the TCs. Although this CSP architecture offers clear advantages, it also has drawbacks, one of which will be detailed in hereafter.

The communication subsystem is composed of a VHF for TM/TC and an S-band, primarily used as high data rate link, but can also be used for TM/TC. The VHF operates in the Short Duration Mission frequency band, created specifically for such missions by the International Telecommunication Union (ITU) in 2019. PRETTY is the first ESA mission to use this band and if not the first, among the first European or even worldwide CubeSats. To comply with the strict power-flux density (PFD) limitations imposed by ITU, the bandwidth of the Space-to-Earth link had to be artificially increased. This has the major disadvantage of making the link more susceptible to external noise sources (as will be detailed in the next section). The VHF is using omnidirectional low-gain antennas and is operated in a half-duplex mode at a nominal data rate of 9.6 kbps. The configuration provides a healthy link margin of 9.4 dB at 5 deg elevations, which is highly desirable for a robust TM/TC link. As mentioned above, using CSP to send TCs and receive TMs on the RF link does not have only advantages. By design, CSP has a large overhead resulting in only ~14% useable bits to store data. The S-band is a high power SDR coupled to a high-gain patch antenna and can offer up to 2 Mbps of data rate. If it is primary used as a high data-rate link to download payload data and logged TMs, it can also be used for TM/TC and hence offers a redundant link to the VHF. When operated using CSP commands, the same overhead applies and only ~14% of the data rate is usable. However, direct IP link can be established between the ground station and the S-band or the payload OBC, in which case a much higher data rate can be obtained [4].
The ADCS finally is composed of a dedicated OBC executing the dedicated off-the-shelf software as well as logging the ADCS specifics TMs. The sensor suit is composed of 6 photo diodes mounted on the solar panels (for which a specific software layer was developed by TUG to read the photodiodes values), a fine sun sensor (FSS), a MEMS magnetometer, and a MEMS gyroscope. The actuator suit is composed of four reaction wheels (RWs) mounted in a tetrahedron configuration as well as three magnetorquers (used for the RWs offloading and detumbling).

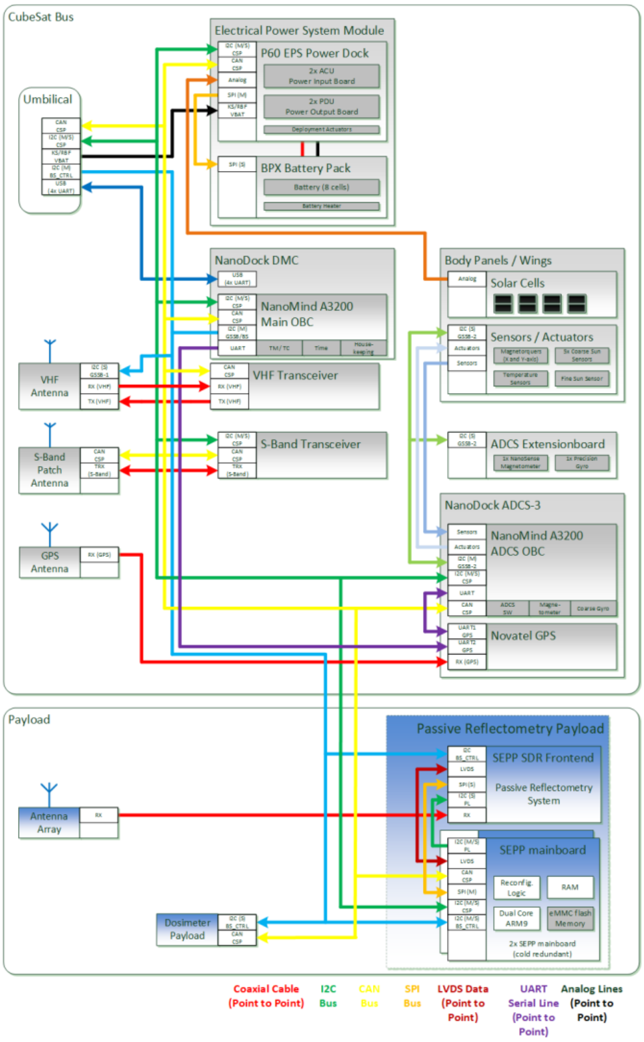

Figure 3 C&DH architecture.

2.2 GNSS-R Payload

The GNSS-R payload design originates from the PARIS IoD study. The goal is to apply the interferometric method in space. This method uses the direct signal from the GNSS transmitter and correlates it with the reflected signal from earth surface. In addition, PRETTY supports the clean replica approach, where a replica of the transmitted code is generated locally on-board. This allows to compare both approaches from the same instrument in space. In Figure 4 an overview of the signal processing is shown. Not shown is the correction of the Doppler, which is necessary to get a correlation result. The GNSS-R payload produces a high-resolution complex waveform, a high-resolution power waveform and a Delay-Doppler Map (DDM, 66 Taps, 9 Frequencies) concurrently for the tracked reflection event. The data is stored on the payload as netCDF file for easy post-processing on ground.

The measurement geometry was chosen so that both, the direct and reflected signal, are within the antenna beam on one side of the satellite. This implies that the elevation angle is very low (5 to 15 degrees, hence incidence is between 75 and 85 degrees). The transmitted signal of GNSS satellites is Right Hand Circular Polarized (RHCP). At these low elevation angles, the polarization does not change, hence a single polarized antenna array is sufficient to retrieve the direct and reflected signal. In Figure 5 the geometry is depicted (Note: distances and angles are not to scale).

The GNSS-R payload consists of two sSatellite eExperimental pProcessing pPlatforms (SEPP) in cold redundancy, an SDR radio frontend [5] and a two -patch antenna. The antenna pattern is designed so that both, the direct GNSS signal and the reflected GNSS-R signal can be received with only one antenna array.

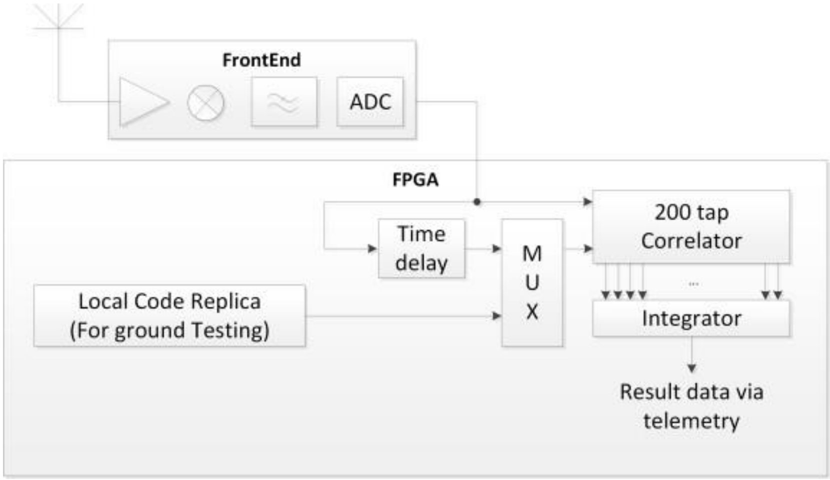

Figure 4 GNSS-R Signal processing overview

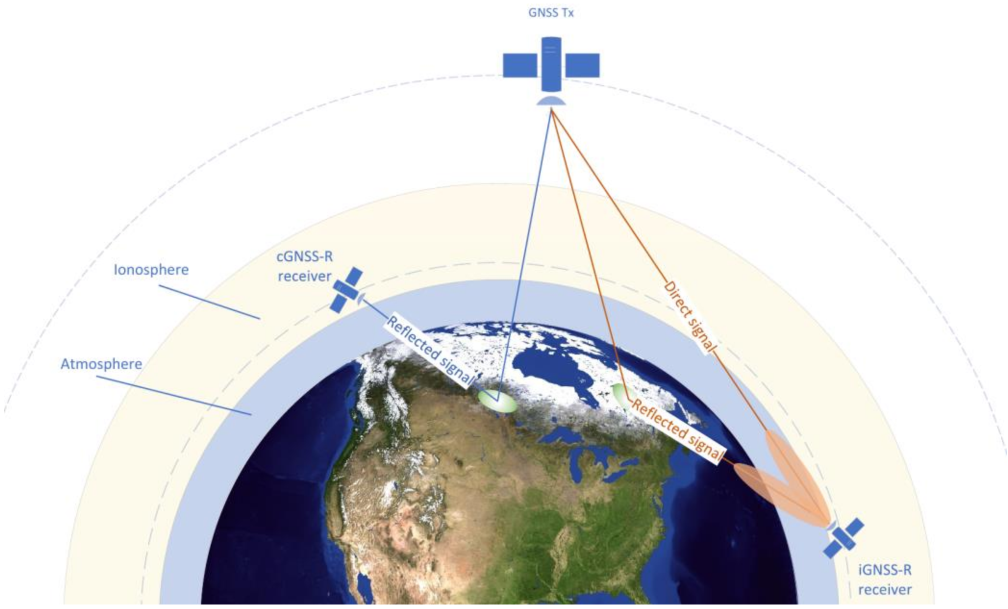

Figure 5 GNSS-R Geometry

For this reason, the antenna pattern is broadened in a vertical direction with the earth as reference. In the horizontal direction, the pattern is kept narrow to detect as little distortion as possible. These two signals are digitised by the SDR and processed inside the FPGA in order to generate two beams, one for the direct signal and one for the reflected signal. The pointing of the satellite is so that the antenna surface is pointing in halfway between the direct and the reflected signal. The beams are steered so that the peak gain is maximized for the direct and reflected signal. The Satellite Experimental Processing Platform (SEPP) is a highly integrated high performance processing platform developed by TU Graz for advanced space applications. The SEPP is realized on a very compact printed circuit board (PCB) design with optimal form factor for CubeSat and Nanosatellite missions. Outstanding computational power is achieved by the use of an Altera Cyclone V SX System-on-Chip (SoC) digital logic device with a built-in dual core ARM A-9 CPU with 800 MHz clock rate and a Cyclone V Field

Programmable Gate Array (FPGA). An in-depth discussion of the GNSS-R payload can be found in [6].

2.3 SATDOS

SATDOS, PRETTY’s second payload, is a new development by Seibersdorf Laboratories. SATDOS is a miniaturized dosimeter payload platform for total ionizing dose (TID) and single event effect (SEE) assessment in-orbit. It is designed for SmallSat applications, such as CubeSats, to assess the effects of the space radiation environment on the satellite’s electronics.
Onboard PRETTY, SATDOS gathers space radiation environment data from the Van Allen Radiation Belts, focusing on three main objectives: (1) evaluating the mission’s total ionizing dose (TID), (2) monitoring in-orbit dose rates, and (3) detecting Single Event Effects (SEE).

- **Total Ionizing Dose (TID) Assessment:** SATDOS plays a pivotal role in assessing the overall radiation dose received by the PRETTY satellite during its one-year mission. This capability is essential for evaluating the impact of radiation on electronic components and ensuring the reliability of satellite systems.
- **Continuous Dose Monitoring:** SATDOS provides continuous monitoring of dose rates in orbit. The recorded data enable comprehensive mapping of the Earth's radiation environment, revealing temporal and spatial characteristics of space weather and facilitating responses to events such as solar storms.
- **Single Event Effects (SEE) Detection**: SATDOS incorporates a single event upset (SEU) monitoring system comprising commercial Static Random-Access Memories (SRAMs) characterized by the European Organization for Nuclear Research (CERN). Two distinct SRAM types are employed to differentiate between particles of varying energies, allowing for the assessment of SEE induced by low-energy protons.

Figure 6 Photo of SATDOS, PRETTY’s reference dosimeter payload.

The platform consists of dedicated analog data conversion, data storage, and communication interfaces integrated with the onboard computer (OBC) of PRETTY. Key components include power bus switches, DC/DC converters, a constant current source, a switching circuit, a temperature sensor, and three radiation sensor types: RADFET, floating gate dosimeters (FGDOS), and SRAMs.
RADFET and FGDOS sensors are utilized to evaluate TID, with variations including shielded and unshielded configurations to discern electron and non-electron contributions to TID. RADFETs offer robust, daily dose monitoring capabilities, while FGDOS sensors provide fine-grained dose rate mapping with short integration times, enhancing spatial resolution along the satellite's trajectory.
The SEE assessment system utilizes commercial SRAMs characterized for radiation susceptibility by CERN and RADSAGA. The differences in response to low-energy protons between the two selected SRAM types enable investigation into the contribution of such particles to the in-orbit SEE rate. An in-depth description of the SATDOS payload can be found in [7].

3 PLATFORM IN-ORBIT PERFORMANCES

After a successful launch on VEGA VV23, PRETTY was inserted into a 560 km Sun Synchronous Orbit (SSO). Early Two-Lines Elements (TLEs) provided by the launch authority are usually low accuracy and more precise ones available on CelesTrak [8], usually take a few days to be available. It is hence not surprising that first passes are of poor quality due to the miss-pointing of the ground station antenna. It is hence only almost 24 hours after launch that the first signs of life of PRETTY were received on ground (in the forms of a few pings). This pointing inaccuracy should not have mattered considering VHF antennas have by design a wide half-power beamwidth. With less than 50% of successful passes, it became quickly evident that ground or space-based interferences were preventing successful communications. Thanks to the support from the SATNOGS community, and in particular the Fachhochschule Wiener Neustadt (FHWN), we could quickly identify that the ORBCOMM constellation was using similar frequencies for their downlink. In fact, within the 137-138 MHz band, identified for short duration missions, the sub-band 137.175-137.825 MHz is also allocated to the Mobile-satellite service (space-to-Earth) on a primary basis, under which Orbcomm operates. The allocated frequencies and a waterfall plot of a concurrent Orbcomm/PRETTY pass is shown in Figure 7 PRETTY VHF being by design more susceptible to noise due to the spread bandwidth (see previous section), as well as due to the significant transmit RF power used by the Orbcomm, it became quickly evident that the ground stations would not be able to hear PRETTY if an ORBCOMMORBOCCM satellite with a neighbouring frequency was above as the same time. To mitigate this impact, it was decided to actively change PRETTY's down-link frequency within the allocated bandwidth during the passes to increase the separation with ORBCOMM ORBOCOMM satellites. This has significantly improved the quality of the link, although it is also clear that ground-based interferences are significant in this frequency band and contribute to the overall poor link quality. This has of course negatively impacted the commissioning, which could be concluded on 5 April 2024.

At 9.6 kbps, the effective data throughput has been computed to be on average ~0.174 kBps. Such a low data rate has been a significant bottleneck for the overall commissioned, especially for the ADCS one, which required extensive TM points over several obits until 3-axis pointing could be achieved. Following this, the ground satiation could be actively tracked by the spacecraft and S-band communication made available. The S-band SDR can be configured to baud rates between 0.5 and 2 MBdps. A rate at 1.5 MBdps was eventually selected as it allows closing the link reliably at 10 deg elevations whilst offering a good effective data throughput. With an average of 22 min access time per day, this setting allows downloading ~127 MB daily (using the IP link, not CSP).

Figure 8 shows the power generation and battery state of charge (SoC). The peak power generation observed in orbit is ~31W when doing sun pointing (a conservative value of 28W was used in the power analysis). When going out of eclipse, a transient can be observed in the battery charging current, before dropping back to zero and then starting to charge the battery again. This phenomenon is not fully understood but is suspected to be related to the MPPT start up. The overall power generation then decreases as the battery SoC reaches 100%. On Figure 8, the average current consumption is ~330mA and corresponds to having powered ON the OBC, GNSS, ADCS, VHF (Rx mode), and GNSS-R payload (idle mode or data transfer mode). When a GNSS-R experiment is carried out, the battery SoC reaches ~31.6V, well within the maximum 50% depth of discharge (DoD) acceptable when doing the experiment (a much smaller DoD is tolerated outside of experiment windows to preserve battery capacity).

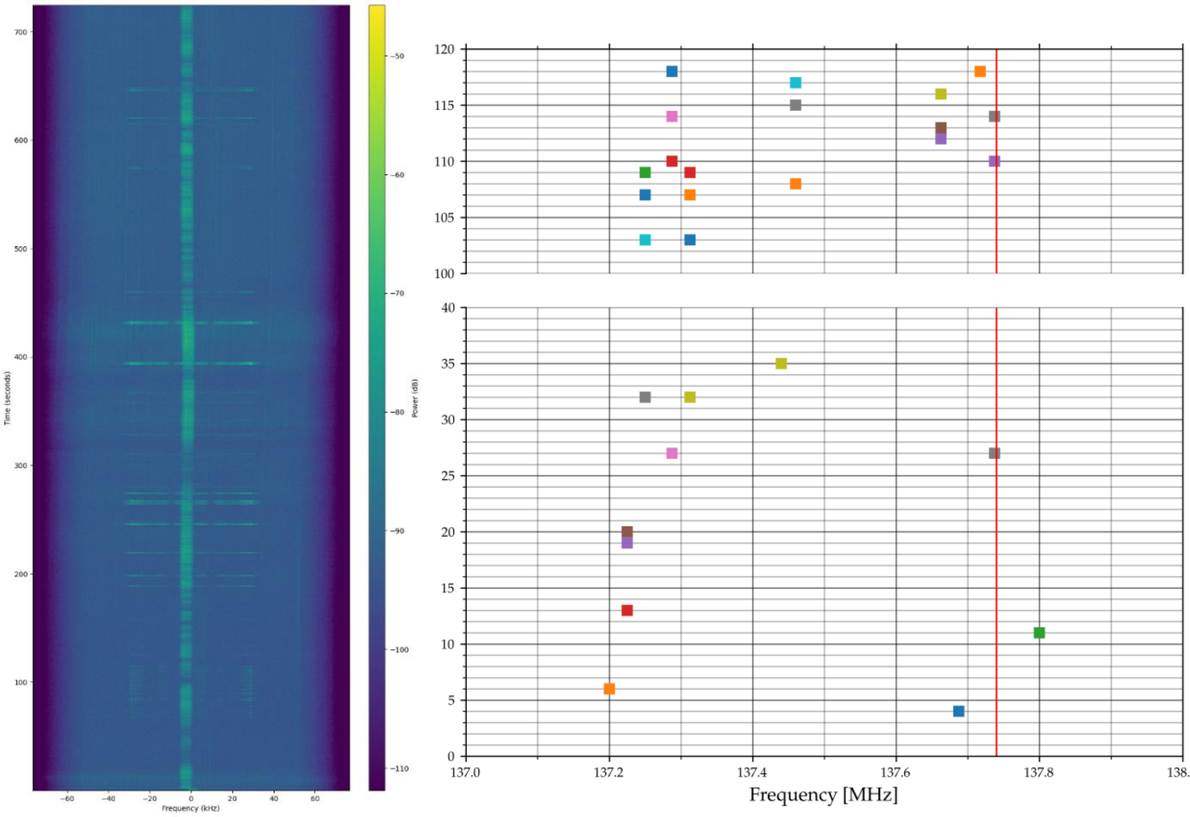

Figure 7 Left: waterfall cart showing an ORBCOM signal (central continuous line) and PRETTY's signal [9]. Right: ORBCOMM satellite number and associated frequency. The red line is PRETY's downlink frequency.

Temperatures in orbit have been on the high side compared to the prediction made by the thermal analysis. The route cause will be fully investigated by the post-flight review, after nominal operations. This warm platform is not concerning as all subsystems are well withing their operational temperatures. There is a concern regarding the battery temperature which shall not exceed 45 deg when charging, as it could otherwise lead to capacity degradation or even failure in the worst case. Three different attitudes have been compared in terms of power generation versus battery temperature and are shown in Figure 9. As can be seen, all three modes are power positive however lead to radically different maximum temperatures (~20 ºC for a tumbling spacecraft, ~40 ºC in Sun Pointing, and ~38 ºC in orbital pointing – min drag). Hence, to mitigate thermal effects on the batteries which could lead to a premature capacity reduction, the CONOPS shown in Figure 10 is being implemented as part of the nominal operations. Due to these higher than anticipated temperatures, additional FDIR rules have been created. Critical subsystems/equipment temperatures and/or up time are now actively monitored by the OBC. When a limit is reached, appropriate actions are undertaken, such as powering off the relevant equipment or triggering a safe mode. This implementation was only possible thanks to the additional software layer for the FDIR that was mentioned in the previous section.

Before reaching a state to capture the GNSS-R payload first light, a tuning of the ADCS was required. Once appropriate stability and control errors were reached and that good tracking performances could be demonstrated during ground station passes, a first acquisition was carried out (see section 4.1). To optimise the overall pointing performance, this payload first light was executed in sunlight so that the FSS could be used in the Kalman filter. Eventually, the aim is to carry out GNSS-R in eclipse to minimise atmospheric disturbances on the GNSS signals caused by the Sun. To this end, a test in eclipse was then carried out and the reaction wheels speed and control error for this test are provided in Figure 11.

Figure 8 Power generation and battery SoC.

Figure 9 Battery SoC and Temperature for (left) tumbling, (centre) sun pointing, right (orbital pointing – minimum drag).

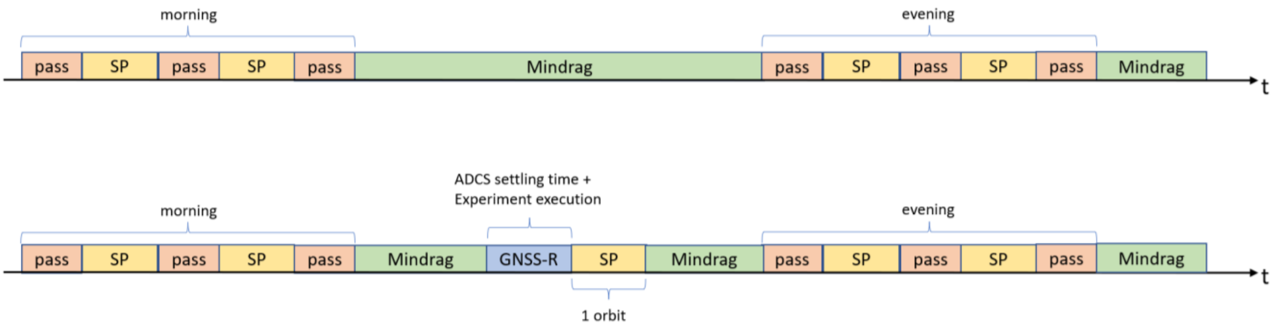

Figure 10 TUG Operations schedule, “pass” means ground station pass, “SP” means Sun Pointing, “Mindrag” indicates orbital pointing with drag minimisation, “GNSS-R” indicates the reflectometry experiment.

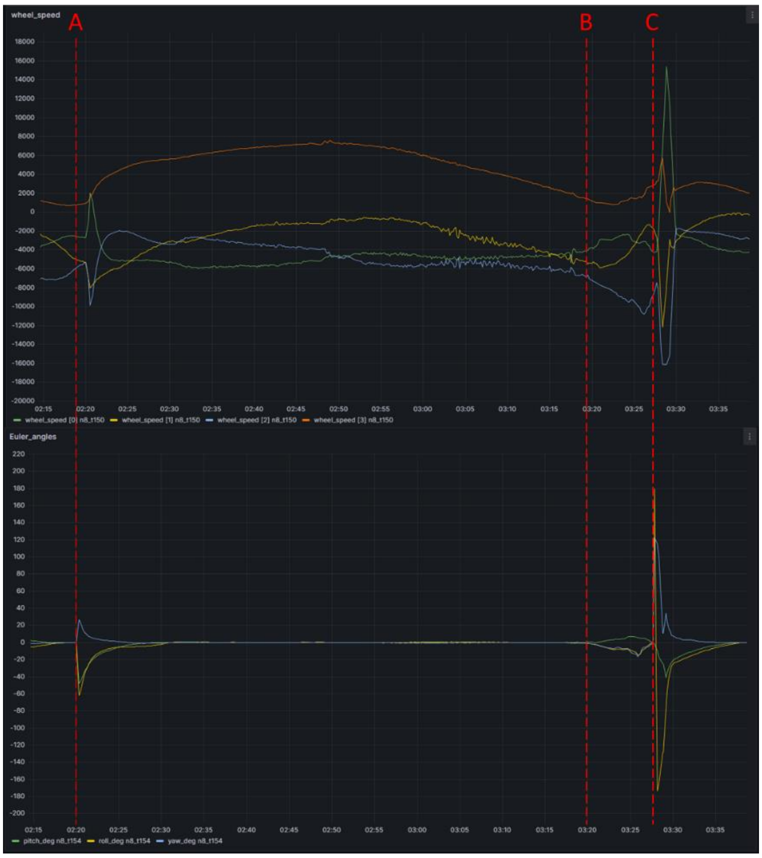

Figure 11 GNSS-R experiment in eclipse – reaction wheels RPM and control error (Euler angles). A) transition from Sun pointing to the attitude to track the reflection point when the experiment starts. B) Start of the experiment, S/C slews to track the reflection. C) End of experiment and transition to Sun pointing. Note: large errors when changing attitude (points A and C) are caused by an instantaneous change of the reference quaternion.

When the experiment starts and the slew is initiated, the control error grows up to ~17 deg, which even without considering the Kalman filter errors (that cannot be quantified in orbit), is largely above the required 9 deg absolute pointing error. Thankfully, the margins accounted for in the payload design are sufficient to compensate for this pointing error and the experiment was successful, nonetheless. The reason for this large error when slewing is likely caused by a too large weight of the magnetometer in the Kalman filter compared to the gyroscope, leading to conflicting estimation of the quaternion and gyro bias. This important weight of the magnetometer in the estimator was initially chosen thinking it would provide good quality measurements. However, strong hard and soft iron effects, as well as internal dipoles generated by the various subsystems are likely to degrade its in-orbit performances. This is supported by the fact that when doing sun pointing (in the ADCS, the Sun direction used for the guidance is not obtained by the Sun sensors but by an internal ephemeris) and using the FSS and magnetometer, the pointing to the sun maxes out to ~9 deg (using the FSS Sun vector to compute the angle to sensor boresight). When disabling the magnetometer, this error drops to <1 deg, as shown in Figure 12.
Despite these larger than anticipated pointing errors, the GNSS-R payload can be used to its full extent and is delivering promising scientific results. The ADCS fine tuning will be continuing throughout the nominal operations to try maximising the signal-to-noise ratio of the scientific data.

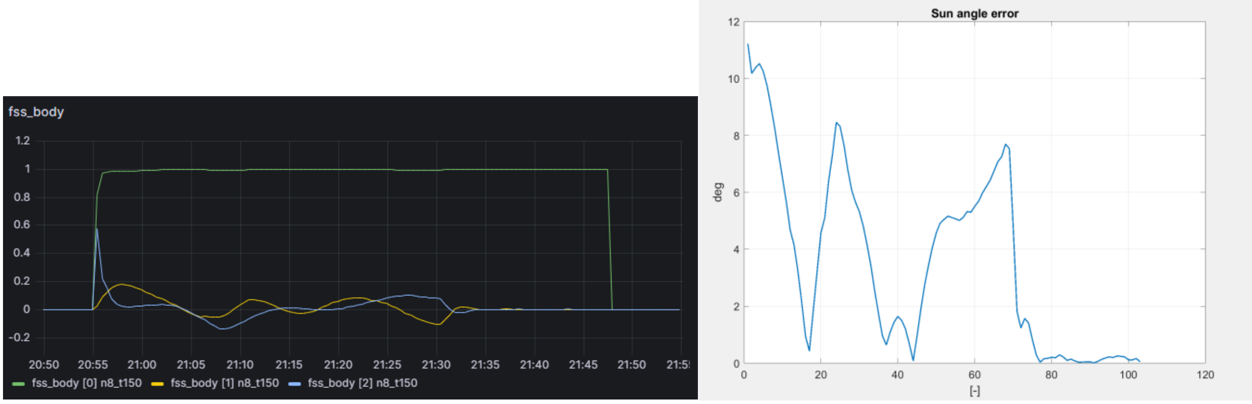

Figure 12 Left: FSS measured Sun vector. Right: Associated Sun angle to FSS boresight (should be 0 deg).

4 PAYLOADS FIRST LIGHTS

4.1 GNSS-Reflectometer

Considering that the reflection loss of the reflected signal depends on the surface, and is about 3dB less over ice than open ocean, the first light acquisition was scheduled to be in the arctic region. We received the first data on the 15. February 2024 from the GNSS-R payload. The integration time on-board the spacecraft was set to 20ms, which is a good compromise between generated data and expected coherence of the signal (i.e. has a direct impact on the Signal to Noise ratio). In Figure 13 the first light acquisition can be seen after post-processing. The coherent integration time was increased to 100ms (i.e. coherently summing up 5 in-space measurements) in order to increase the SNR further. The incoherent integration time (i.e. summing up the power values of the incoherent data) was set to 2s, which flattens the noise floor and makes the peak come out more clearly. The data shown is from the high-resolution complex waveform. PRETTY has a Digital Elevation Map integrated, which is used for the calculation of the reflection point. The height profile (upper right plot) shows the used height for calculation of the reflection point, i.e. the expected height. Three areas can be distinguished in the lower right plot, first where no reflection is visible (mostly blue), second at the top of the plateau (5:30:15) we see peaks in a vertical line and third in the horizontal direction (~5:30:20 to 5:31:15) a high SNR coming out from the noise.
Taking a closer look at the first reflection peak at around 5:30:15, which starts on the lower left of the Sentinel data, one can see the evaluation of the DDM over different surface areas. The first DDM is before reaching the ice surface (hence no data), the next two DDM show a single peak centered at 0Hz Doppler (this indicates a mirror like reflection, which is expected over pure ice). The next three DDM (lower row) show lots of correlation peaks for different delays and doppler frequencies. However, at the same position as the peak in the previous DDM, a peak is also visible in the lower row. This corresponds to a change in the color of the Sentinel image, which could indicate sea ice (Note: This has still to be confirmed, but it's very likely that PRETTY has tracked pure ice and the change to sea ice).
Regarding the visible peaks in the vertical direction, our first guess is they are coming from interference from Distance Measuring Equipment (DME) for aviation. These signals are transmitted from ground stations, in order to find the distance of an aircraft. The peak power of these signals is around 1kW. In [10] the typical pulse shape and the effect on the correlation waveform is shown. In order to verify the assumption, the GNSS-R paylaod was put in the so called RAW mode, where it stores the incoming ADC samples on-board (I and Q samples for both antenna patches simultaneously with full 12bit resolution). In Figure 15

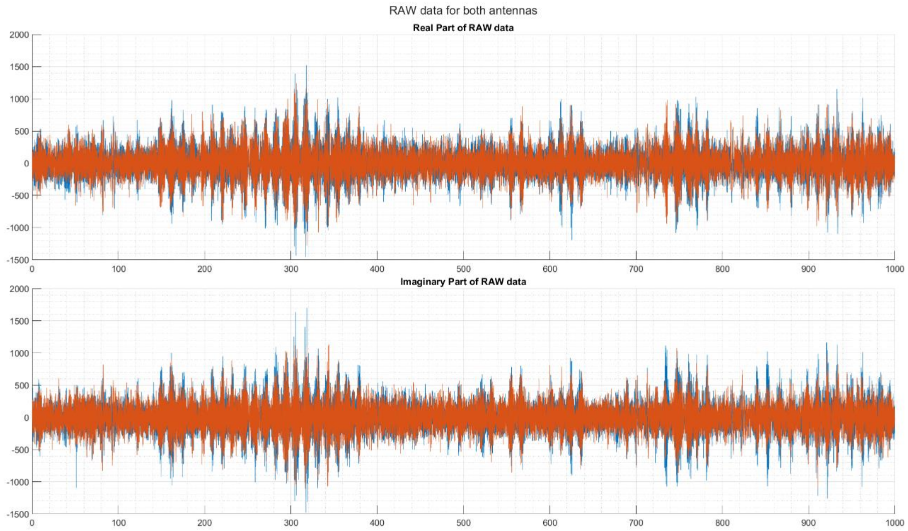

the data captured can be seen. The position of PRETTY was over the Atlantic and was basically surrounded by DME stations. The pulse shape matches those of DME pulses very well.

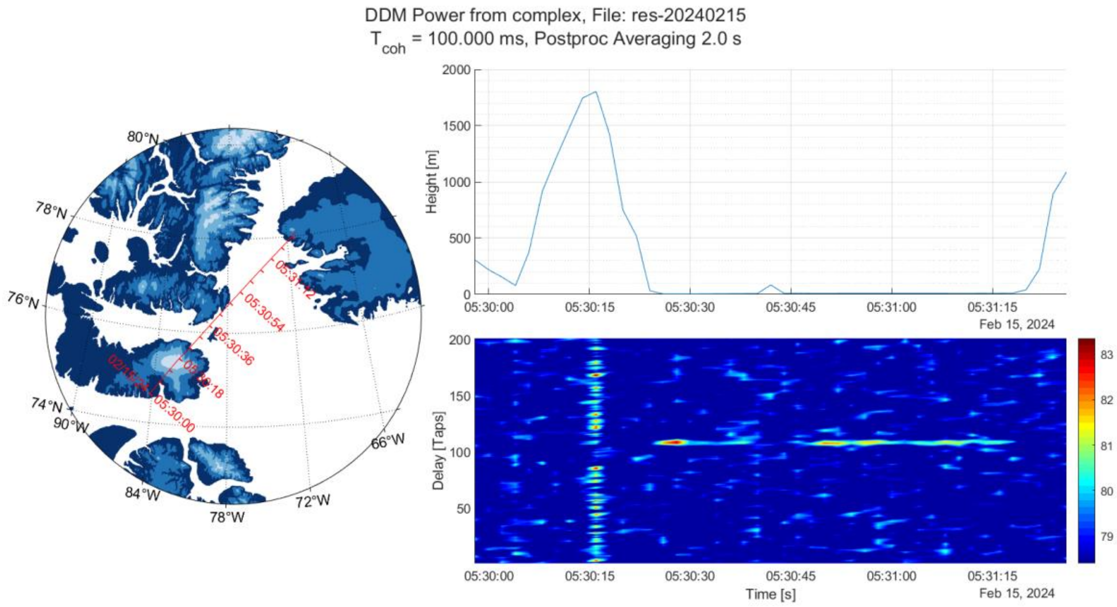

Figure 13 First Light from GNSS-R payload after post-processing.

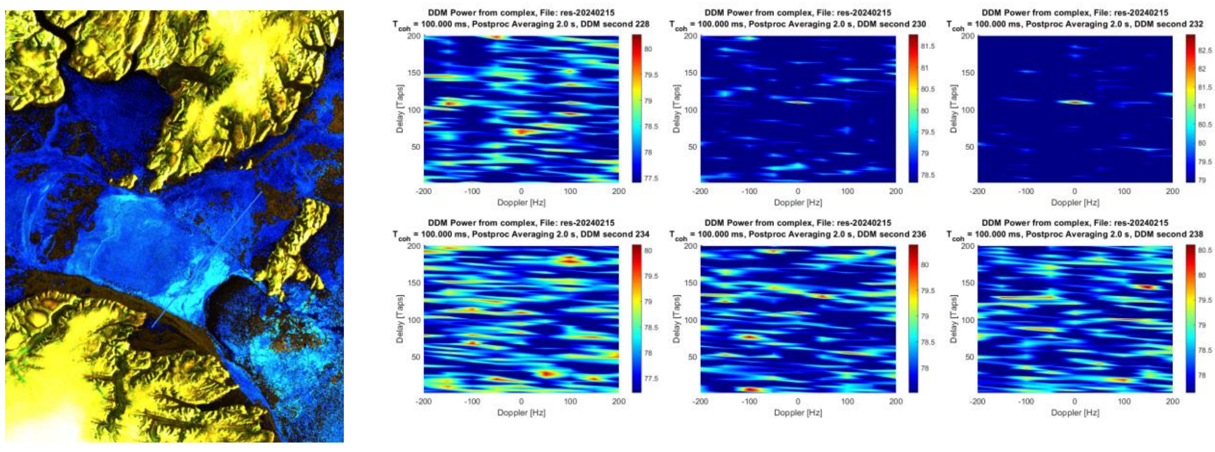

Figure 14 DDM for first Light from GNSS-R payload after post-processing, left: Sentinel-1 data with ground track in blue, right: corresponding DDM.

Such interferences would drastically reduce the ability for the GNSS-R payload to produce meaningful results. However, during the development and the switch to the L5 frequency band, we decided to implement the so-called “Pulse blanking” technique inside the FPGA. The incoming signal power is measured with a moving average filter, and once a threshold (which is configurable by our GNSS-R software) is reached, the complete pulse is blanked, i.e. set to 0. Hence, they do not contribute to the correlation result. The fine-tuning of the threshold will be done during nominal operations.

4.2 SATDOS

During the commissioning phase of the PRETTY CubeSat mission, the SATDOS payload conducted its first comprehensive in-orbit data collection spanning approximately 29 hours. This dataset offers a detailed insight into the radiation environment encountered by the satellite, regarding accumulated total ionizing dose (TID), in-orbit TID rate, and Single Event Effects (SEE).

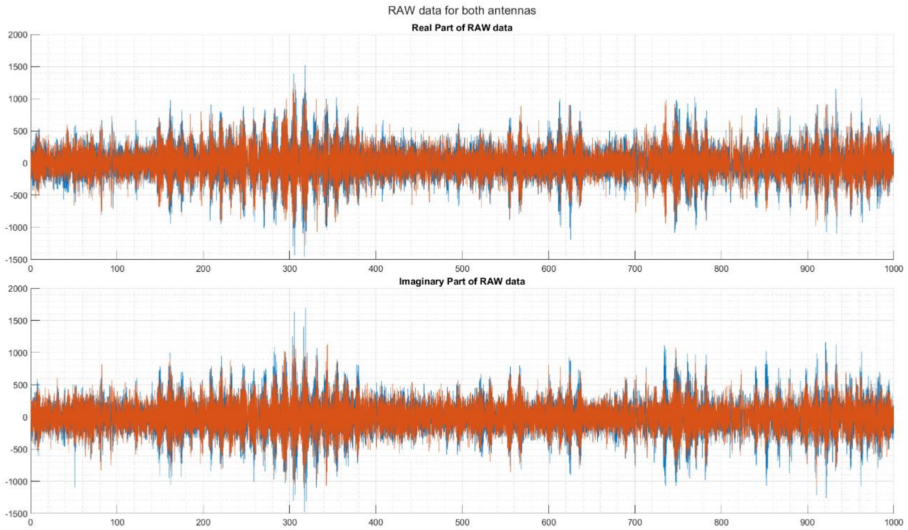

Figure 15 RAW data captured.

- **Total Ionizing Dose (TID) Assessment:** SATDOS, equipped with RADFET and FGDOS sensors, provided a thorough evaluation of TID accumulation over the observation period. The data revealed an accumulated dose of approximately 0.4 rad, demonstrating the payload's capability to quantify radiation exposure in space. Notably, both shielded and unshielded FGDOS sensors exhibited consistent TID contributions, suggesting predominant proton radiation sources. Conversely, RADFET sensors showed no significant increase in total dose for the first 29 hours of data, consistent with their minimum resolution of approximately 1 rad. This uniformity across sensors underscores SATDOS's reliability in assessing TID variations in orbit.
- **Total Ionizing Dose (TID) Rate:** The observed in-orbit dose rate remained below 2 mrad/s throughout the observation period, indicative of relatively stable radiation conditions.
- **Single Event Effects (SEE) Detection:** One of the significant milestones achieved during the commissioning phase was the detection of Single Event Upsets (SEU) by SATDOS. And indeed, during the only 29 hours of commissioning phase data of SATDOS, we observed a first bit-flip on the Cypress SRAM.

Comparing the in-orbit data with simulation results based on ECSS standard models confirmed that our results are in-line with the simulated in-orbit response and the current episode of solar maximum conditions.

The initial 29-hour dataset from SATDOS aboard the PRETTY CubeSat represents a significant milestone in quantifying the effects of the space radiation environment on the satellite's electronics. Through comprehensive TID assessment, dose rate monitoring, and SEE detection, SATDOS demonstrates its efficacy in evaluating radiation hazards and ensuring the reliability of satellite systems. Moving forward, continued data collection and analysis will further enhance our understanding of space radiation dynamics and inform the development of robust mitigation strategies for future CubeSat missions.

5 CONCLUSION

On 5 April 2024, PRETTY commissioning was declared successful and nominal operations have started. The spacecraft will be operated until October 2024, at which point it will either be passivated for its end of life or operations be extended pending funding availability. The platform is performing as per its specifications and allows the payloads to carry out their nominal operations and deliver the sought scientific data. Some issues have been encountered on the VHF link (interferences caused by the Orbcomm satellites) and the platform is overall warmer than anticipated. For both issues, a way forward has been identified and implemented for the nominal operations. The ADCS is unfortunately not yet delivering performances meeting the GNSS-R payload pointing requirements. Despite this issue, the excellent payload design still allows to carry out the measurements. This is largely due to the design margins that were kept as required throughout the project life cycle and are being used to day to their full extent.

REFERENCES

[1] A. J. Hörmer *et al.*, "PRETTY – A CubeSat mission for passive reflectometry and dosimetry." International Astronautical Federation, IAF, p. 56144, Jan. 01, 2020. Accessed: Apr. 15, 2024. [Online]. Available: https://graz.elsevierpure.com/en/publications/pretty-a-cubesat-mission-for-passive-reflectometry-and-dosimetry

[2] A. J. Hörmer *et al.*, "The PRETTY CubeSat system redundancy concept." 2021. Accessed: Apr. 15, 2024. [Online]. Available: https://graz.elsevierpure.com/en/publications/the-pretty-cubesat-system-redundancy-concept

[3] "GitHub - libcsp/libcsp: Cubesat Space Protocol - A small network-layer delivery protocol designed for Cubesats." Accessed: Mar. 27, 2024. [Online]. Available: https://github.com/libcsp/libcsp

[4] A. J. Hoermer and M. Wenger, "Performance Evaluation and Comparison of VHF and S-Band Communication Links for the PRETTY Spacecraft (in publication process)," in *2024 14th International Symposium on Communication Systems, Networks and Digital Signal Processing, CSNDSP 2024*,

[5] R. Zeif, A. J. Hörmer, M. Henkel, M. Kubicka, M. Wenger, and O. F. S. Koudelka, "The Pretty Software Defined Radio System And Its Use As Communication Platform In Space." Mar. 10, 2018. Accessed: Apr. 15, 2024. [Online]. Available: https://graz.elsevierpure.com/en/publications/the-pretty-software-defined-radio-system-and-its-use-as-communica

[6] A. Dielacher, H. Fragner, O. Koudelka, A. Dielacher, · H Fragner, and · O Koudelka, "PRETTY-passive GNSS-Reflectometry for CubeSats PRETTY-passive GNSS-

Reflektometrie für CubeSats Schlüsselwörter GNSS-Reflektometrie · CubeSat · Erdbeobachtung · In-Orbit-Demonstration,” *Elektrotech. Inftech*, vol. 139, pp. 25–32, 2022, doi: 10.1007/s00502-022-00993-7.

[7] C. Tscherne *et al.*, “Development of a Miniaturized Reference Dosimeter Payload for SmallSat Applications,” *RADECS 2021 - European Conference on Radiation and its Effects on Components and Systems*, 2021, doi: 10.1109/RADECS53308.2021.9954463.

[8] “CelesTrak: Current GP Element Sets.” Accessed: Mar. 28, 2024. [Online]. Available: https://celestrak.org/NORAD/elements/

[9] “SatNOGS Network - Observation 8533121.” Accessed: Mar. 28, 2024. [Online]. Available: https://network.satnogs.org/observations/8533121/

[10] R. Onrubia, J. Querol, D. Pascual, A. Alonso-Arroyo, H. Park, and A. Camps, “DME/TACAN impact analysis on GNSS reflectometry,” *IEEE J Sel Top Appl Earth Obs Remote Sens*, vol. 9, no. 10, pp. 4611–4620, Oct. 2016, doi: 10.1109/JSTARS.2016.2556745.